SIEMENS

Reprint

Full-field digital mammography with grid-less acquisition and software-based scatter correction: Investigation of dose saving and image quality

Andreas Fieselmann, Daniel Fischer, Ghani Hilal, Frank Dennerlein, Thomas Mertelmeier, and Detlev Uhlenbrock

Full-field digital mammography with grid-less acquisition and software-based scatter correction: Investigation of dose saving and image quality*

Andreas Fieselmann[1], Daniel Fischer[1], Ghani Hilal[2], Frank Dennerlein[1], Thomas Mertelmeier[1], and Detlev Uhlenbrock[3]

[1] Siemens AG, Healthcare Sector, Erlangen, Germany; [2] University of Düsseldorf, Düsseldorf, Germany;
[3] University of Bochum, Bochum, Germany and St.-Josefs-Hospital, Dortmund, Germany

Abstract

Anti-scatter grids used in full-field digital mammography not only attenuate scattered radiation but also attenuate primary radiation. Dose saving could be achieved if the effect of scattered radiation is compensated with a software-based scatter correction not attenuating the primary radiation. In this work, we have carried out phantom studies in order to investigate dose saving and image quality of grid-less acquisition in combination with software-based scatter correction. The results show that similar image quality (contrast-to-noise ratio and contrast-detail visibility) can be obtained with this alternative acquisition and post-processing scheme at reduced dose. The relative dose reduction is breast-thickness-dependent and is >20% for typical breast thicknesses. We have carried out a clinical study with 75 patients that showed non-inferior image quality at reduced dose with our novel approach compared to the standard method.

Keywords: digital mammography, scattered radiation, scatter correction, anti-scatter grid, dose reduction, feature analysis study.

1. Introduction

X-ray mammography requires a high image quality for the detection of subtle features indicating malignant tissue. Scattering is a physical process that degrades image quality.[1] Scattered radiation generates a smoothly varying, noisy background that is added to the image. The varying background signal decreases relative image contrast. Furthermore, the additive noise reduces the contrast-to-noise ratio (CNR).

In mammography reduction of scattered radiation is traditionally achieved by using hardware approaches. Anti-scatter grids are most frequently used. Other approaches include using slot or multislit scanning[2, 3] or applying an air gap.[4] Besides reducing the amount of scattered radiation, anti-scatter grids also attenuate primary radiation. The primary radiation is the radiation that passes through the breast without being absorbed or scattered by the breast tissue. The attenuating effect of an anti-scatter grid is usually expressed in terms of the Bucky factor $B_f = 1/T_t$ with T_t being the total transmission of the grid. $B_f \approx 2$ is a typical value.[5] To compensate for the (unintended) attenuation of primary radiation of the grid a higher entrance dose is necessary.

Since asymptomatic women undergo mammography screening, dose is of highest importance in breast imaging. In order to reduce entrance dose – and therefore also the organ dose – several studies have been carried out that investigate grid-less acquisition for digital mammography.[6-12]

* Fieselmann, A., Fischer, D., Hilal, G., Dennerlein, F., Mertelmeier, T., and Uhlenbrock, D., "Full-field digital mammography with grid-less acquisition and software-based scatter correction: investigation of dose saving and image quality," In: Proceedings of SPIE Medical Imaging 2013: Physics of Medical Imaging, Lake Buena Vista, FL, USA, vol. 8668, pp. 86685Y, (2013), doi:10.1117/12.2007490

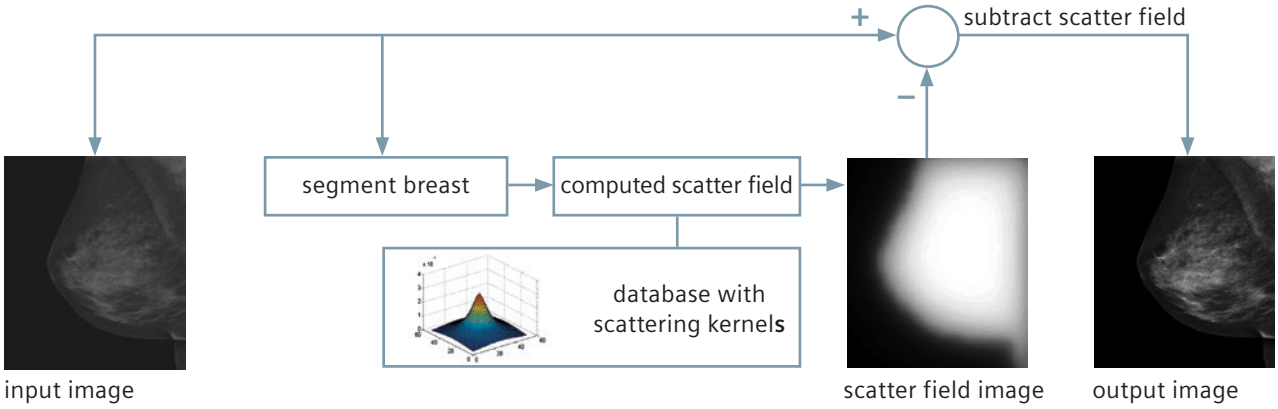

Figure 1. Simplified illustration of the software-based scatter correction.

In a subset of these studies software-based scatter correction (SBSC) has been included as an image post-processing step.[9-12] With SBSC it is possible to mitigate the effect of scattered radiation by software-based methods instead of hardware methods. SBSC can particularly reduce the varying background signal caused by the scattered radiation. The additive noise due to scatter is of stochastic nature and it can be compensated by the relative increase in primary radiation.

These studies suggest a potential for dose reduction with uncompromised image quality for grid-less mammography. E. g., Gennaro et al.[8] did not use SBSC and state that dose saving by 15–25% was possible for PMMA equivalent breasts thinner than 40 mm. Tromans et al.[12] used SBSC and state that dose can be reduced by 37–49% for their phantoms tested (e. g. CIRS BR3D phantom). Although these studies show very promising results no clinical study in this field has been carried out yet. In our work, we present our novel approach for grid-less acquisition and SBSC. We evaluated our approach using phantom-based measurements and a clinical study with 75 patients.

2. Software-based scatter correction

The measured radiation without grid consists of primary and scattered radiation. The scattered radiation can be modeled by a low-frequency and a high-frequency component. The low-frequency component generates a smoothly varying additive offset to the intensity values in the image. The high-frequency component is basically additive noise.

The purpose of the SBSC is to estimate the low-frequency component and subtract it from the measured image. Note that the decrease of the CNR due to the high-frequency component of the scattered radiation can be compensated by the increased transmission of primary radiation for the case of the grid-less acquisition.

We apply a scatter correction algorithm* for full field digital mammography (FFDM) that estimates the scatter field depending on the object using 2D scatter kernels and convolution.[13, 14] Scatter kernels representing local scatter fractions were generated by Monte Carlo simulations based on object properties and the geometry and acquisitions parameters (e. g., anode/filter combination, tube voltage) of a commercially available FFDM system (MAMMOMAT Inspiration; Siemens AG, Healthcare Sector, Erlangen, Germany). Figure 1 shows a simplified illustration of this algorithm.

The total computation time for the scatter correction is short (of the order of seconds) and the usual workflow during screening mammography is not affected due to waiting times.

* The technology is not available in all countries. Due to regulatory reasons its future availability cannot be guaranteed.

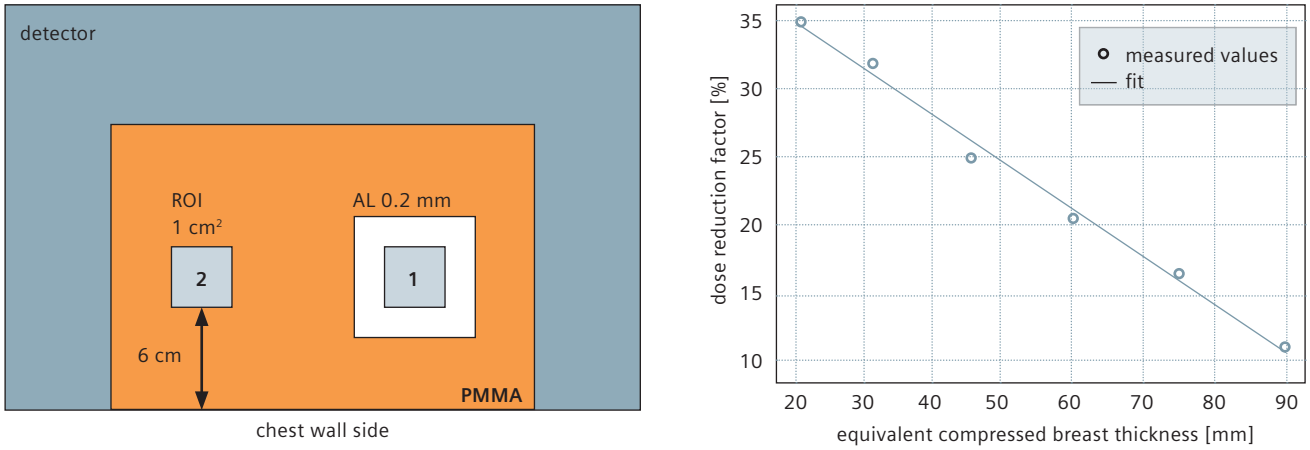

(a) experimental set-up

(b) results

Figure 2. Experimental set-up and results of the CNR measurement.

3. Phantom Study

We have carried out phantom experiments in order to address the following two questions:

1. What relative dose reduction can be achieved with grid-less acquisition and SBSC compared to a standard acquisition (with grid) while providing the same CNR in the image?

2. When using grid-less acquisition and SBSC at this reduced dose level, how does the contrast-detail visibility[15] of these images compare to those images acquired in standard mode (with grid)?

3.1 Material and methods: contrast-to-noise ratio measurements

Investigating CNR is relevant for grid-less acquisition due to the high-frequency noise component of scatter. We measured CNR for different polymethyl methacrylate (PMMA) plate thicknesses according to the EUREF guidelines.[15] PMMA plates of thickness between 20 and 70 mm in steps of 10 mm were placed on the detector of a MAMMOMAT Inspiration as illustrated in Figure 2a. An aluminium (AL) foil of 0.2 mm thickness was placed on top of the PMMA plates.

First an image with grid was acquired in standard automatic exposure control mode. Then the grid was removed and a set of images was acquired using the same beam quality (filter/anode combination, tube voltage) but with varying exposures from 100% to about 50% of the exposure of the first image. Note that the exposure could be varied in certain discrete steps only. In each image (both acquisition modes, all PMMA thicknesses) two regions of interest (ROIs), one being inside and one being outside of the position of the AL-foil (Figure 2a), were used to compute the CNR corresponding to that image.[15]

For each PMMA thickness we determined the exposure which yields the same CNR with a grid-less acquisition compared to the acquisition with grid. A fit of the squared CNR values versus exposure was used for determining precise exposure values. Thus, for each PMMA thickness two exposure values exist which provide the same CNR for acquisitions with and without grid, respectively. From the two exposure values a PMMA-thickness-dependent dose reduction factor for grid-less acquisition was computed. This procedure was performed separately without and with SBSC.

The results for a specific PMMA thickness were converted to an equivalent compressed breast thickness using the conversion table presented in Dance et al.[16]

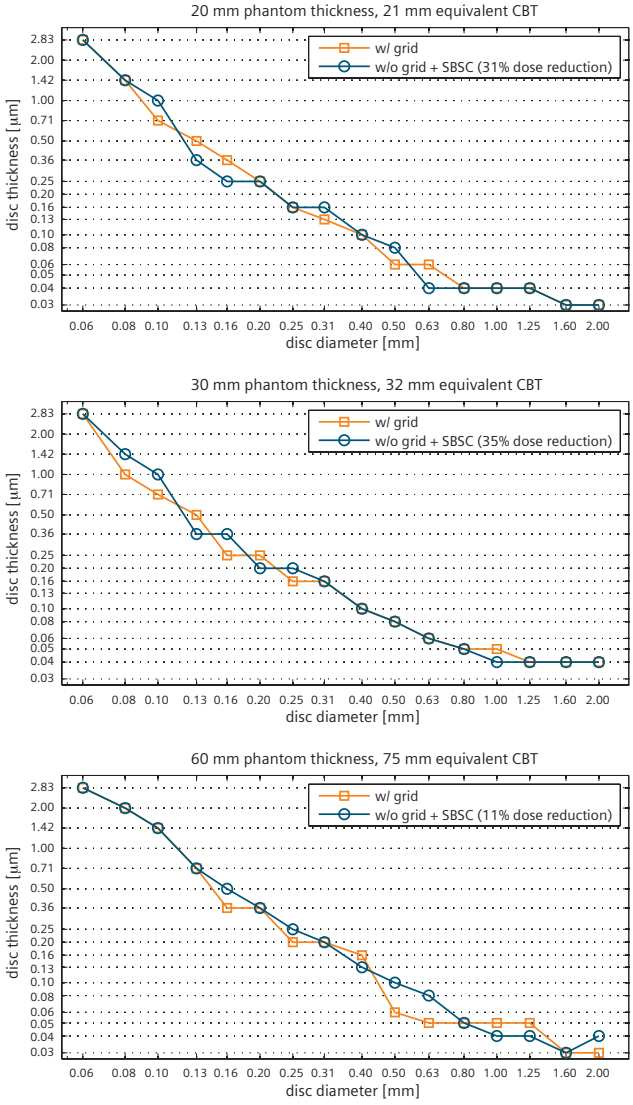

Figure 3. Log-log plots of contrast-detail curves of the acquisitions with grid and without grid and SBSC at reduced dose level for different equivalent compressed breast thicknesses (CBT).

3.2 Material and methods: contrast-detail measurements

We used the feature plate of the CDMAM 3.4 phantom (Artinis Medical Systems B.V., AS Zetten, the Netherlands) in order to measure the contrast-detail curves[15] of images acquired with and without grid. For the latter case the images were acquired using the same beam quality but at a reduced dose according to the results from the previous CNR measurements. PMMA blocks were used to generate different phantom thicknesses (20–70 mm in steps of 10 mm) that simulate different equivalent compressed breast thicknesses. See again Dance et al.[16] for the conversion factors. The feature plate itself is equivalent to 10 mm PMMA. The evaluation of the CDMAM phantom images was performed with the automatic scoring software CDCOM.[17] Eight images were acquired for every phantom thickness, processed by CDCOM and contrast-detail curves were determined.

3.3 Results

Figure 2b shows the dose reduction factors (DRF) as a function of equivalent compressed breast thickness (CBT) with an additional linear fit ($|r| > 0.99$, $p < 0.001$). The DRF fit has a slope of –0.34%/mm. The results for the DRF without SBSC are similar (the slope of the fit is –0.37%/mm). Representative contrast-detail curves for three different phantom thicknesses are shown in Figure 3.

3.4 Discussion

The measured DRF are monotonously decreasing and can be very well modeled by a linear function. The dependence of the DRF on the breast thickness will be explained next. With increasing breast thickness the scatter fraction[18] and the amount of additive noise due to scatter increases. A certain amount of the additional primary radiation – due to removal of the grid – is needed to compensate for this noise. Thus less additional primary radiation is available to compensate for the lower dose. In order to provide the same CNR the dose cannot be reduced by the same factor for thicker breasts compared to thinner breasts. The contrast-detail curves of the acquisitions with and without grid are generally very similar indicating that similar image quality can be obtained using the two different acquisition approaches. The higher relative dose reduction for 30 mm PMMA thickness (35%) compared to 20 mm PMMA thickness (31%) is due to the limited, discrete choice of values when selecting the exposure parameters for the manual acquisition without grid.

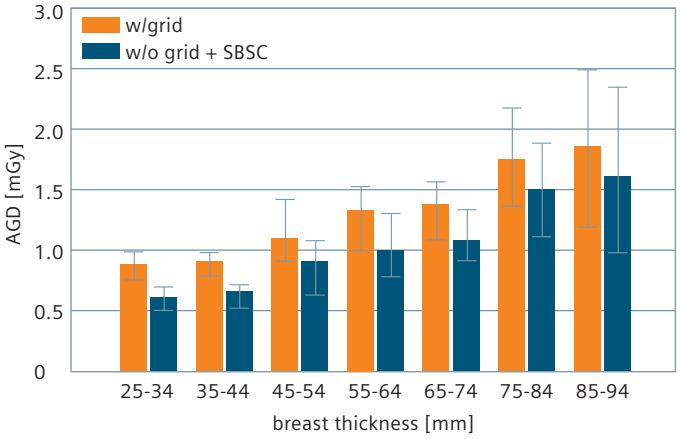

Figure 4. Average glandular dose in the clinical study (error bars represent 1 standard deviation).

category	mean	SD	*p*-value
overall comparison of image quality	0.07	0.31	$< 10^{-14}$
diagnostic certainty: mass	0.12	0.30	$< 10^{-13}$
diagnostic certainty: microcalcification	0.08	0.42	$< 10^{-07}$
diagnostic certainty: architectural distortion	0.18	0.28	$< 10^{-07}$
visibility of tissue near the edge of the breast	0.00	0.16	$< 10^{-24}$
visibility of structures in the pectoral muscle	0.09	0.29	$< 10^{-10}$
visibility of noise	0.01	0.22	$< 10^{-17}$

Table 1. Results for the reading study comparing image pairs on the 7-point scale (SD: standard deviation). Positive mean values indicate better impression with the grid-less technique with SBSC.

4. Clinical Study

We have carried out a clinical feature-analysis study in order to investigate the grid-less acquisition and SBSC with reduced dose under realistic clinical conditions.

4.1 Material and methods

75 female patients were enrolled in this clinical study who had been recalled for further diagnostic mammograms after screening. The clinical study has been approved by the ethics committee. Informed written consent to participate in this study was obtained from all patients.

For each patient, two exposures were made during the *same* compression phase. The breast side and the laterality (CC or MLO) were randomly chosen. The first exposure was made in standard automatic mode with grid. The second exposure was made without grid and with reduced dose. The dose was reduced by lowering the tube current-time product according to the factors determined in the phantom experiment (Figure 2b) and keeping the other acquisition parameters constant. The images acquired without grid were processed with the SBSC described in Section 2 before processing them using standard mammographic image processing algorithms.[19]

The image pairs were evaluated by five radiologists each having more than five years of experience in interpreting mammograms. In a blinded side-by-side reading of the image pairs, the radiologists had to compare the images on a 7-point scale (–3,–2, . . . , +3) according to the following seven categories:

1. overall image quality
2. diagnostic certainty: mass
3. diagnostic certainty: microcalcification
4. diagnostic certainty: architectural distortion
5. visibility of tissue near the edge of the breast
6. visibility of structures in the pectoral muscle
7. visibility of noise

After the *blinded* reading the ratings were transformed onto a 7-point scale where positive values indicate preference of the grid-less technique with SBSC. Based on biostatistical considerations and previous (unpublished) studies, non-inferiority of the grid-less technique is assumed for a rating > –0.3 points on the 7-point scale.

4.2 Results

The study population is characterized as follows. The mean age of the women was 56.5 ± 5.5 years (50 to 72 years). The mean compressed breast thickness was 57.5 ± 14.7 mm (28 to 87 mm). The distribution of mammographic findings in the study population was: masses (57%), microcalcifications (41%), architectural distortions (20%). Note that multiple findings per patient were possible. The breast density in the study population was rated as: ACR 1 (4%), ACR 2 (53%), ACR 3 (33%), ACR 4 (10%).

Figure 4 shows the distribution of the average glandular dose (AGD) in the study population. The absolute AGD reduction averaged over all patients was 0.26 ± 0.06 mGy. The relative AGD reduction ranges from 12% (breast thickness 85–94 mm) to 32% (breast thickness 25–34 mm).

The results from the reading study are shown in Table 1. In this table, positive mean values indicate a preference for the grid-less acquisition with SBSC. All mean values are close to zero. The *p*-values corresponding to a one-sided t-test (a = 0.025) with threshold set to –0.3 are shown as well. Using this t-test, statistical significant non-inferiority of the grid-less technique in combination with SBSC has been shown ($p < 0.001$).

One pair of images from the clinical study is presented in Figure 5 (39 mm breast thickness, 27% relative dose reduction).

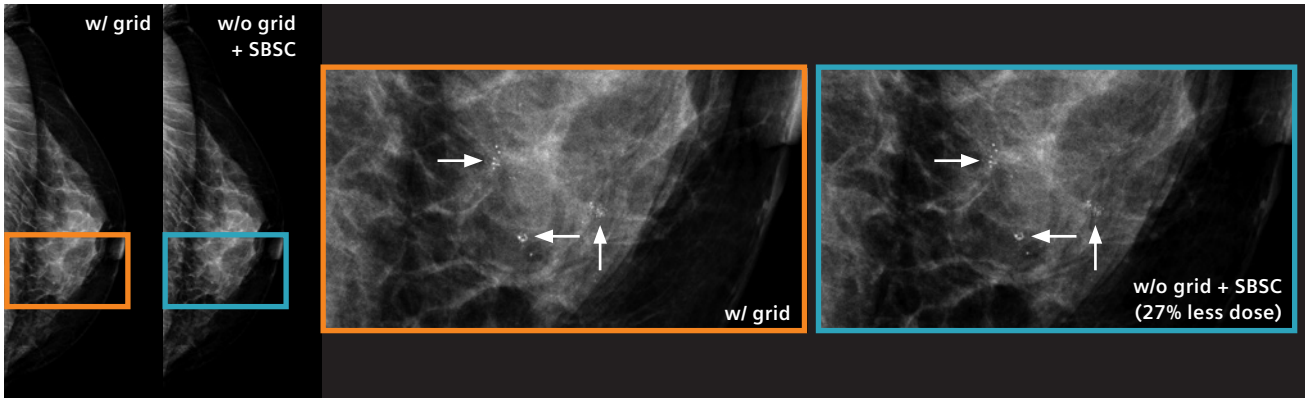

Figure 5. Example images from the clinical study with a magnification of a region of interest containing microcalcifications (marked with arrows). The image without grid and SBSC was acquired with 27% less dose (0.76 mGy instead of 1.04 mGy) compared to the image acquired in standard mode with grid.

4.3 Discussion

In the clinical study, the relative, breast-thickness-dependent dose reduction obtained with grid-less mammography with SBSC is very similar to that obtained in the phantom study. Differences may be due to the limited, discrete choice of exposure values that can be selected in manual exposure mode. Interestingly, the average absolute reduction of AGD (0.26 mGy) is similar across breast thickness ranges. A dose increase is necessary for thicker breasts which – in combination with the decrease of relative dose reduction for thicker breast – leads to this similar absolute value.

It is important to assess the image quality at the reduced dose with grid-less mammography and SBSC. The ratings by the radiologists have mean values close to zero. This is actually an indicator for the same image quality. The main results of the clinical study is that statistically significant non-inferiority of the grid-less technique with SBSC can be shown.

5. Summary

Patient dose in X-ray mammography is a highly relevant topic. In our work, we presented an investigation regarding the dose saving potential of grid-less FFDM in combination with SBSC. Dose can be reduced with grid-less mammography due to a relatively higher amount of primary radiation reaching the detector. We have carried out phantom studies to investigate the dose saving potential and image quality. In order to test our technique under realistic conditions we conducted a clinical study which showed non-inferiority of this approach compared to the standard approach. The relative dose reduction is breast thickness dependent and varies between 12% for the thicker breasts (85–94 mm) and 32% for the thinner breasts (25–34 mm) in the study.

References

[1] Bushberg, J. T., Seibert, J. A., Leidholdt, E. M., and Boone, J. M., [*The Essential Physics of Medical Imaging*], Lippincott Williams & Wilkins, Philadelphia, PA, 3rd ed. (2012).

[2] Shen, S. Z., Bloomquist, A. K., Mawdsley, G. E., Yaffe, M. J., and Elbakri, I., "Effect of scatter and an antiscatter grid on the performance of a slot-scanning digital mammography system," *Medical Physics* **33**(4), 1108–1115 (2006).

[3] Åslund, M., Cederström, B., Lundquist, M., and Danielsson, M., "Scatter rejection in multislit digital mammography," *Medical Physics* **33**(4), 933–940 (2006).

[4] Krol, A., Bassano, D. A., Chamberlain, C. C., and Prasad, S. C., "Scatter reduction in mammography with air gap," *Medical Physics* **23**(7), 1263–1270 (1996).

[5] Salvagnini, E., Bosmans, H., Struelens, L., and Marshall, N. W., "Quantification of scattered radiation in projection mammography: Four practical methods compared," *Medical Physics* **39**(6), 3167–3180 (2012).

[6] Veldkamp, W. J. H., Thijssen, M. A. O., and Karssemeijer, N., "The value of scatter removal by a grid in full field digital mammography," *Medical Physics* **30**(7), 1712–1718 (2003).

[7] Diekmann, F., Diekmann, S., Berzeg, S., Bick, U., Fischer, T., and Hamm, B., "Dose reduction through gridless technique in digital full-field mammography," *Fortschritte Röntgenstrahlen* **175**, 769–774 (2003). (article in German).

[8] Gennaro, G., Katz, L., Souchay, H., Klausz, R., Alberelli, C., and di Maggio, C., "Grid removal and impact on population dose in full-field digital mammography," *Medical Physics* **34**(2), 547–555 (2007).

[9] Baydush, A. H. and Floyd, C. E., "Improved image quality in digital mammography with image processing," *Medical Physics* **27**(7), 1503–1508 (2000).

[10] Nykänen, K. and Siltanen, S., "X-ray scattering in full-field digital mammography," *Medical Physics* **30**(7), 1864–1873 (2003).

[11] Xia, J., Floyd, C., Lo, J., and Harrawood, B., "Improved signal to noise in full-field digital mammography by replacing the anti-scatter grid with nonlinear image processing," in [*Proceedings of the Radiological Society of North-America (RSNA) 2004*], (2004). (unpublished).

[12] Tromans, C. E., Cocker, M., and Brady, S. M., "Digital scatter removel for mammography and tomosynthesis image aquisition," in [*Proceedings of the 11th International Workshop on Digital Mammography (IWDM) 2012*], **7361**, 260–267 (2012).

[13] Rührnschopf, E.-P. and Klingenbeck, K., "A general framework and review of scatter correction methods in x-ray cone-beam computerized tomography. Part 1: Scatter compensation approaches," *Medical Physics* **38**(7), 4296–4311 (2011).

[14] Rührnschopf, E.-P. and Klingenbeck, K., "A general framework and review of scatter correction methods in cone beam CT. Part 2: Scatter estimation approaches," *Medical Physics* **38**(9), 5186–5199 (2011).

[15] Perry, N., Broeders, M., de Wolf, C., Törnberg, S., Holland, R., von Karsa, L., and Puthaar, E., eds., [*European Guidelines for Quality Assurance in Breast Cancer Screening and Diagnosis*], Office for Official Publications of the European Communities, Luxembourg, 4th ed. (2006).

[16] Dance, D. R., Young, K. C., and van Engen, R. E., "Further factors for the estimation of mean glandular dose using the United Kingdom, European and IAEA breast dosimetry protocols," *Physics in Medicine and Biology* **54**(14), 4361–4372 (2009).

[17] Young, K. C., Alsager, A., Oduko, J. M., Bosmans, H., Verbrugge, B., Geertse, T., and van Engen, R., "Evaluation of software for reading images of the CDMAM test object to assess digital mammography systems," in [*Proceedings SPIE Medical Imaging 2008: Physics of Medical Imaging*], **6913**, 69131C (2008).

[18] Mertelmeier, T. and Bernhardt, P., "Scatter in digital mammography: antiscatter grid versus slot-scanning," in [*Proceedings SPIE Medical Imaging 2005: Physics of Medical Imaging*], **5745**, 299–306 (2005).

[19] Zanca, F., Jacobs, J., Ongeval, C. V., Claus, F., Celis, V., Geniets, C., Provost, V., Pauwels, H., Marchal, G., and Bosmans, H., "Evaluation of clinical image processing algorithms used in digital mammography," *Medical Physics* **36**(3), 765–775 (2009).

Not for distribution in the USA.

On account of certain regional limitations of sales rights and service availability, we cannot guarantee that all products included in this brochure are available through the Siemens sales organization worldwide. Availability and packaging may vary by country and are subject to change without prior notice. Some/All of the features and products described herein may not be available in the United States.

The information in this document contains general technical descriptions of specifications and options as well as standard and optional features which do not always have to be present in individual cases.

Siemens reserves the right to modify the design, packaging, specifications, and options described herein without prior notice. Please contact your local Siemens sales representative for the most current information.

Note: Any technical data contained in this document may vary within defined tolerances. Original images always lose a certain amount of detail when reproduced.

Please find fitting accessories:
siemens.com/medical-accessories

Siemens Healthcare Headquarters
Siemens Healthcare GmbH
Henkestr. 127
91052 Erlangen
Germany
Phone: +49 9131 84-0
siemens.com/healthcare

Order No. A91XP-30005-23E1-7600 | Printed in Germany | CC 3807 05161. |

siemens.com/healthcare